

Article

The Effect of Heat- and Salt Treatment on the Stability and Rheological Properties of Chickpea Protein-Stabilized Emulsions

Diana Mańko-Jurkowska ^{1,*}  and Ewa Domian ² 

¹ Department of Chemistry, Institute of Food Sciences, Warsaw University of Life Sciences, 02-776 Warsaw, Poland

² Department of Food Engineering and Process Management, Institute of Food Sciences, Warsaw University of Life Sciences, 02-776 Warsaw, Poland; ewa_domian@sggw.edu.pl

* Correspondence: diana_manko-jurkowska@sggw.edu.pl

Abstract: The aim of the study was to evaluate the effect of heat- (95 °C) and/or salt (0.1 M NaCl) treatment on the physical stability and rheological properties of oil-in-water emulsions stabilized with chickpea protein concentrates (CPCs) for various purposes. Thus, the particle size distribution (PSD), shear behavior, and long-term Turbiscan stability of the prepared emulsions were examined. The oscillatory (dynamic) measurements were also performed to obtain information on the viscoelasticity of tested fluids during thermal treatment. The obtained results indicated that the emulsion stabilized with gelling CPC (eC_g) was Newtonian fluid with a homogeneous structure, but susceptible to creaming. Heat-treated eC_g exhibited a sol–gel transition at 86 °C and formed fine-stranded aggregates without affecting stability. In turn, heat-induced gelation of eC_g in the presence of 0.1 M NaCl resulted in the formation of an aggregated, spatial gel network, stabilization of the system, and a significant change in both shear rheological properties and PSD. Contrariwise, emulsions stabilized with standard CPC (eC_s) were unstable heterogeneous systems containing both fine particles < 1 μm and coarse particles of about 100 μm, exhibiting shear-thinning and yield stress. The heat-induced viscoelasticity of eC_s was reversible, while heat- and salt-treated emulsions did not form a gel.

Keywords: chickpea protein; protein-stabilized oil-in-water emulsion; emulsion stability; emulsion rheology



Citation: Mańko-Jurkowska, D.; Domian, E. The Effect of Heat- and Salt Treatment on the Stability and Rheological Properties of Chickpea Protein-Stabilized Emulsions. *Appl. Sci.* **2024**, *14*, 2698. <https://doi.org/10.3390/app14072698>

Academic Editor: Leonel Pereira

Received: 2 February 2024

Revised: 12 March 2024

Accepted: 21 March 2024

Published: 23 March 2024



Copyright: © 2024 by the authors. Licensee MDPI, Basel, Switzerland. This article is an open access article distributed under the terms and conditions of the Creative Commons Attribution (CC BY) license (<https://creativecommons.org/licenses/by/4.0/>).

1. Introduction

For environmental, health, social, and ethical reasons, plant proteins are of great interest in the food industry as suitable candidates for replacing proteins of animal origin (e.g., whey proteins, casein, and gelatin) in new product formulations [1,2]. They are particularly appreciated by consumers because they are natural, “green”, “vegan-friendly”, and sustainable for the environment and agriculture [3]. Among all alternative protein sources, the use of legume proteins in the food sector is rapidly expanding. Legumes are being considered as more environmentally friendly alternatives to meat, poultry, and dairy products as they have low greenhouse gas and water footprints but also enrich the soil through nitrogen fixation. They are nutrients with an exceptionally high protein content compared to other plant-based protein sources. Furthermore, legumes are abundant, low-cost, sustainable, not highly allergenic, and widely acceptable by consumers [2,4].

Chickpea (*Cicer arietinum* L.) is a nutrient-rich food and the second most consumed pulse worldwide [5,6], but the use of its protein preparations in the food industry is still limited. This is mainly due to the fact that their properties and how they interact within food matrices were scarcely studied, especially compared to other legume proteins such as soybean or pea proteins [7]. Both the emerging interest in chickpea proteins as a matrix in functional foods [8,9] and the fact that chickpeas are not only a sustainable protein source but also contribute to soil health and climate resilience [5,10] prompted us to use these proteins in the present study.

Chickpea is a valuable source of high-quality protein rich in a number of essential amino acids (e.g., lysine, leucine, and arginine), including branched-chain ones [2]. The methionine content in chickpea proteins is relatively low compared to animal-based proteins, making it the limiting amino acid. However, chickpea protein can still play a crucial role in a well-balanced plant-based diet [11].

The main chickpea proteins are salt-soluble globulins (53–60%), in which the ratio of legumin (16S) and vicilin (7S) fractions is six to one. The legumin fraction has higher sulfur-containing amino acids (e.g., cysteine and methionine) than vicilins, while vicilins do not contain cysteine residues and therefore cannot form disulfide bonds [12–15].

Chickpea and aquafaba (the viscous liquid that can be drained from canned or cooked chickpea) proteins have been reported to be nutrients with a wide range of useful techno-functional properties, such as foaming, emulsification, and gelling [6,16–19]. These properties are affected by the solubility of proteins and their molecular state in an aqueous media (native, partially denatured, denatured, aggregated) [20–22]. It is known that external conditions such as pH, ionic strength, and temperature can control protein solubility by influencing protein–water and protein–protein interactions. There is a strong pH dependence for chickpea protein solubility. They have minimal solubility in the pH range of 4.0–5.0; above pH 6.5, all proteins have a solubility greater than 70% [23], while the maximum solubility of chickpea proteins was reported at acidic (<3.0) and alkaline (>8.0) pH [19].

Protein solubility is also affected by the presence of salt ions. Typically, at a low salt concentration regime, protein solubility increases along with salt concentration (“salting-in”) because the charged biomolecules are surrounded by the salt’s counterions, and this screening results in a decrease in the electrostatic free energy of the protein and an increase in solvent activity. However, at a high salt concentration regime, solubility decreases with increasing salt concentration (“salting-out”) as protein and salt ions compete to interact with the solvent molecules [20,24].

Protein solubility generally enhances with increasing temperature up to ~50 °C, where proteins tend to rearrange their secondary and tertiary structures, resulting in hydrophobic amino acids (e.g., those with free sulfur or thiol groups) becoming available. At higher temperatures, cross-linking between unfolded protein molecules (hydrophobic and electrostatic protein–protein interactions, hydrogen bonds, and sulfhydryl–disulfide exchanges) leads to their aggregation, precipitation, sedimentation, or gelation depending on their thermal stability [20,25].

Knowledge about the impact of environmental conditions on the functional properties of proteins is used, among others, in the production of protein powders for specific applications; because depending on the method of preparation, they may differ in functional properties [14]. The native structure of proteins is frequently destroyed by the harsh conditions of extraction and recovery in large-scale production, which can cause them to unfold, denature, and aggregate. Even partial denaturation can reduce the solubility of proteins in water and adversely affect their techno-functional properties [2,15,26,27].

The low solubility of proteins in solutions can be improved using physical, chemical, or enzymatic approaches [20,28,29]. High-pressure homogenization (HPH) has attracted much attention as a promising non-thermal, physical technique. HPH is environmentally friendly, does not require chemicals, does not affect the nutritional properties of proteins, and can be used both to water protein dispersions and protein-stabilized emulsions to improve their dispersibility [22,25]. This technique was used, among others, in the case of legume proteins derived from soy [30], lentil [31], or faba bean [32] in order to improve their solubility and/or modify their functional, structural, and rheological properties.

In our previous studies [33,34], we have shown that the number of cycles of the emulsion passing through the HP homogenizer can affect the properties of the protein-stabilized emulsion. This time, not only the emulsions but also their water protein dispersions were pre-processed in the HP homogenizer. After preliminary tests, the effects of heat- (95 °C) and salt (0.1 M NaCl) treatment, applied simultaneously and separately, on particle size distribution, shear behavior, and long-term Turbiscan stability were examined for emul-

sions prepared with two commercial chickpea proteins concentrates, standard CPC and CPC with gelling functionality. The oscillatory (dynamic) measurements were performed to obtain information on the viscoelasticity of the tested emulsions during heating and then cooling and to better understand the causes of emulsion instability under the influence of environmental conditions.

2. Materials and Methods

2.1. Materials

All the materials were used as received. Commercially available chickpea protein concentrates, Cicerpro™ 70G (pH = 7.5) and Cicerpro™ 70S (pH = 6.5) (Exeller, Piaseczno, Poland), were used in this study. According to the manufacturer's declaration, Cicerpro™ 70G has very good gel strength and can be used in many products where such functionality is required. Both CPC powders contain 67% protein (with the same amino acid composition), 20% fat, 5% fiber, max. 8% ash, and <0.2% carbohydrates on a dry basis, according to the manufacturer.

The refined rapeseed oil (Bunge, Kruszwica, Poland) was used as a model oil phase in the prepared emulsions. According to the manufacturer's declaration, 100% refined and cold-filtered virgin oil; liquid at 20 °C; fatty acid composition: 8.4% SAFA, 63.3% MUFA, and 27.5% PUFA. Distilled deionized water was used to prepare all dispersions.

2.2. Preparation of CPC-Stabilized Emulsions

The CPC dispersions containing 3.5% (*w/v*) protein dry matter per batch were prepared in deionized water by agitation at 30 °C for 40 min using a low-speed mechanical blender (Thermomix TM31; Vorwerk, Wrocław, Poland) and kept overnight at 4 °C to allow protein hydration. Sodium azide (0.1% (*w/v*)) was used as a general preservative to avoid microbial contamination.

The next day, the CPC dispersions were processed using a Panda 2K high-pressure (HP) homogenizer (Niro Soavi, Parma, Italy) at 50 MPa and 5 MPa in the first and second stages, respectively. Both dispersions were prepared in two variants for preliminary tests. In the first one, they were passed through the homogenizer once, in the second one, twice. The dispersions prepared on the basis of standard Cicerpro™ 70S (CPC_s) and gelling concentrate Cicerpro™ 70G (CPC_g) were designated as C_s and C_g, respectively.

The C_s and C_g were used to prepare eC_s and eC_g emulsions, respectively. The pre-emulsions (300 mL per batch in duplicate) were prepared using a T18 IKA Ultra-Turrax disperser (Wilmington, NC, USA) at ~10,000 rpm for 5 min, slowly introducing the oil into the CPC dispersion. The oil phase content was fixed at 3.2% as in full-fat milk with a balanced protein concentrate to oil ratio (1:1 (*w/w*)). Then, the pre-emulsions were processed in the HP homogenizer at 50 MPa and 5 MPa in the first and second stages, respectively.

2.3. Stability Tests

The long-term stability of all emulsion systems was evaluated using the Turbiscan Lab Expert optical analyzer (Formulation, Toulouse, France) based on the Turbiscan Stability Index (TSI) and calculated using the TurbiSoftLab2.3.1.15 program.

Immediately after preparing the emulsions, cylindrical glass measuring cells were filled with 20 mL of samples for analysis. The samples were scanned over the entire height of the sample (from 1 to 43 mm) at preset intervals within 28 days. The obtained BS profiles vs. sample height were analyzed in terms of destabilization phenomena monitored through time. BS was calculated according to Equation (1) [35]:

$$BS \approx 1/\sqrt{l^*}, l^*(\phi, d) = 2d/[3\phi(1 - g)Q_s] \quad (1)$$

where l^* is the mean free path of photon transport, ϕ is the volume fraction of the particles, d is the mean diameter of the particles, and g and Q_s are optical parameters given by the Mie theory.

TSI was used to evaluate the stability of the entire dispersion system and was obtained according to Equation (2) [36]:

$$TSI = \sum_i \frac{\sum_h |scan_i(h) - scan_{i-1}(h)|}{H} \quad (2)$$

where $scan_i(h)$ is average backscattering for each time (i) of measurement, $scan_{i-1}(h)$ is average backscattering for the $i - 1$ time of measurement, and H is the height of the sample.

2.4. Rheological Tests

Rheological measurements were performed using a Thermo Scientific™ HAAKE™ MARS™ 40 Rheometer equipped with a CC27 DG Ti double-gap coaxial cylinder geometry at an axial gap of 4 mm. The results were analyzed using the HAAKE RheoWinDataManager V.4.75 software (Thermo Scientific, Karlsruhe, Germany).

Steady shear tests were performed in a controlled-rate mode at a linearly increasing shear rate of 1–100 s⁻¹ for 210 s at 20 °C. Experimental flow curves (shear stress vs. shear rate) were compared using a power law model (Equation (3)), which is a typical equation characterizing shear-thinning fluids:

$$\tau = \tau_0 + k \cdot \dot{\gamma}^n \quad (3)$$

where τ is the shear stress (Pa), k is the consistency index (Pa·sⁿ), $\dot{\gamma}$ is the shear rate (s⁻¹), τ_0 is the yield stress (Pa), and n is the flow index; $\tau_0 \geq 0$ and $n < 1$ for a shear-thinning fluid, while for a Newtonian fluid $\tau_0 = 0$ and $n = 1$.

The oscillation tests were performed in the controlled deformation mode. All measurements were conducted under small-amplitude oscillatory shear, using a set frequency of 5 Hz and a constant strain of 2%, and data were collected every 30 s. The samples of 3 mL were loaded onto the rheometer at 20 °C and held constant for 15 min while collecting rheological data. After the initial equilibrium step, the temperature was increased from 20 to 95 °C at a rate of 4 °C min⁻¹. The temperature was held constant at 95 °C for 15 min and then decreased from 95 °C back to 20 °C at the same 4 °C min⁻¹ rate as the temperature increase step. After the decreasing temperature sweep, the temperature was again held constant at 20 °C for 15 min to complete the full temperature cycle. To prevent evaporation, the sample was covered using an insulated sample hood.

2.5. Particle Size Distribution (PSD)

The emulsion droplet size distribution was measured based on the principle of laser diffraction using a CILAS 1190 particle size analyzer (CILAS, Orléans, France). The refractive index values used were 1.33 for water and 1.46 for the samples, and the absorption index value was 0.001 for all samples. The obscuration in all measurements was kept at ~5% using distilled water as a dispersant.

The characteristic PSD data included mean volume diameter, d_{43} , and *span*. *span* values were calculated according to Equation (4):

$$span = \frac{d_{0.9} - d_{0.1}}{d_{0.5}} \quad (4)$$

where d_x is the average droplet size in the 90th, 50th (median), and 10th percentiles of the cumulative volume distribution of particle size.

2.6. Confocal Laser Scanning Microscopy (CLSM)

The microstructures of the emulsions were observed under the confocal laser scanning microscope (FV3000, Olympus Corporation, Tokyo, Japan). The protein and oil phases were labeled using Nile blue dye (1 mg mL⁻¹ water, excitation/emission wavelengths = 460/546 nm) and Nile red dye (1 mg mL⁻¹ ethanol, excitation/emission wavelengths = 559/578 nm), respectively. A 0.05 mL of fluorescence dyes and 5 mL of emulsion

were mixed, and a drop of sample was placed on the microscope slide, secured with a glass coverslip, and finally imaged using an oil immersion 63× magnification lens.

2.7. Statistical Methods

All measurements were performed for each sample at least in duplicate. The statistical analysis of results was performed with Statistica 13.1 (StatSoft, Kraków, Poland) using options of multivariate analysis of variance (ANOVA) including post hoc test. Differences between mean values were evaluated with the Tukey test at a significance level of $\alpha = 0.05$, with homogeneous groups of mean values denoted by letter classification.

3. Results and Discussion

3.1. The Influence of Pre-Treatment of the Protein Dispersions on the Properties of the CPC-Stabilized Emulsions

Protein-stabilized emulsion formation by homogenization is widely used in both scientific research and the food industry to increase both protein solubility as well as emulsion stability [37]. According to Mulla et al. [38], non-thermal methods like high-pressure or high-hydrostatic pressure processing enhance the rheological, thermal, and functional properties of legume proteins with minimal effect on macro- and micronutrients and properties related to swallowing and digestion. Literature data indicate that both the high pressure and the number of passes through the homogenizer affect the physicochemical and functional properties of emulsions, as well as their stability [33,34,39,40]; but it should be emphasized that HPH-induced effects are strongly dependent on matrix characteristics and treatment conditions [41]. In the protein-stabilized emulsion, as a result of high-pressure treatment, in addition to the reduction in size and homogeneity of the fat globules, there may also be protein unfolding and exposure of some reactive groups, such as free sulfhydryl and hydrophobic groups, thus further enhancing the functionality of proteins [39]. According to Melchior et al. [41], as HPH intensity increased, protein unfolding was favored, leading to increased solubility and oil-holding capacity and consequently to obtaining a novel plant-protein-based ingredient with improved techno-functionalities and digestibility, but over-processing conditions caused further protein aggregation and a general reduction in functionalities.

In the present study, we prepared emulsions in HP homogenizer, but due to the limited solubility of legume proteins in water, it was also examined whether the number of passes of the protein dispersions through the two-stage HP homogenizer (50 MPa and 5 MPa at the first and second stages, respectively) affects the properties of the emulsions.

The particle size distribution (PSD) (in cumulative and histogram forms) of chickpea protein dispersions, C_s and C_g , passed once and twice through an HP homogenizer, is presented in Figure S1a, and the PSD of the eC_s and eC_g emulsions produced using these protein dispersions is shown in Figure S1b. The obtained granulometric curves of C_s and C_g clearly indicated that repeating the homogenization operation resulted in both a shift in PSD towards smaller particles, as well as a change in the shape of the histogram curve (Figure S1a). For C_s , the coarse particle fraction in the range of 20 to 100 μm was redistributed as a result of second homogenization, and the three-modal histogram took a bimodal form with similar values of two modes of the smaller fractions in the range of 1 to 20 μm and 0.1 to 1 μm . The PSD curves of the C_g were characterized by a bimodal shape with the main peak of the finer fraction in the range of 1 to 10 μm and a clear decrease in the modal values as a result of repeated homogenization.

The comparison of the corresponding curves obtained for the emulsions indicated that the PSD of eC_s and eC_g was highly consistent with respect to the protein dispersions, which was illustrated by the similar shape of the granulometric curves. The granulometric curves of the eC_g indicated a strongly monomodal distribution in the $<5 \mu\text{m}$ range. The three-modal PSD of the eC_s showed a fraction of fine particles in the range of 0.1 to 1 μm as well as two fractions of coarse particles in the range of a few to over 100 μm (Figure S1b).

The ANOVA analysis showed that the type of protein concentrate (standard CPC or gelling CPC) turned out to be a factor significantly differentiating all parameters of the PSD, both the protein dispersions and the emulsions (Table S1). On the other hand, the number of passes of the protein dispersion through the HP homogenizer was a factor that significantly differentiated the parameters of PSD only in relation to the protein dispersions. Thus, the use of gelling CPC allowed the production of homogeneous fine emulsions with an average particle size $< 1 \mu\text{m}$, while the use of standard CPC resulted in heterogeneous emulsions, containing both fine particles $< 1 \mu\text{m}$ and coarse particles of about $100 \mu\text{m}$, regardless of the number of pre-homogenization cycles.

3.2. Emulsion Stability

3.2.1. Untreated CPC-Stabilized Emulsions

The Turbiscan tool enables quick identification and monitoring of destabilization mechanisms in emulsion systems [33,34,42]. It detects migration (sedimentation, creaming) or particle size change (coalescence) of a dispersed phase over time, which leads to a variation in backscattering (BS) and transmission (T) of light intensity [43]. The instrument makes it possible to determine and compare the kinetics of destabilization of many samples and to determine the stability parameter—Turbiscan Stability Index (TSI) [33,34,43].

The results of the stability measurements of eC_g and eC_s presented as BS (%) profiles over the entire height of the sample during the 28-day storage are shown in Figure 1 and the TSI kinetics of their global destabilization are presented in Figure S2.

Particle migration was observed in both types of emulsion during the storage period. In the case of eC_g , it was primarily instability due to gravity separation (creaming) accompanied by an increase in BS intensity in the upper part of the emulsion and a decrease in the lower part due to migration of droplets from the bottom of the sample (Figure 1a), while for the eC_s , creaming of the emulsion was accompanied by sedimentation and the increase in BS intensity in the lower part of the sample (Figure 1e).

The long-term stability of emulsion is closely related to the particle size of the internal phase and its distribution [44] but also to the rheological properties of emulsion [45–47]. Firstly, the narrow PSD and small mean droplet sizes are associated with more stable emulsions [48]. This is attributed to the significant effect of droplet size on the gravitational separation of the emulsions [49]. Secondly, proteins as amphiphilic molecules adsorb at internal interfaces, which results in decreasing the interfacial tension as well as the formation of compact, resistant to ruptures, adsorption layers at the surface of the oil, providing repulsive steric and electrostatic interactions between droplets, which avoid their coalescence [47,50]. The rheological properties of adsorbed layers influence the rheology of an emulsion as a whole [46].

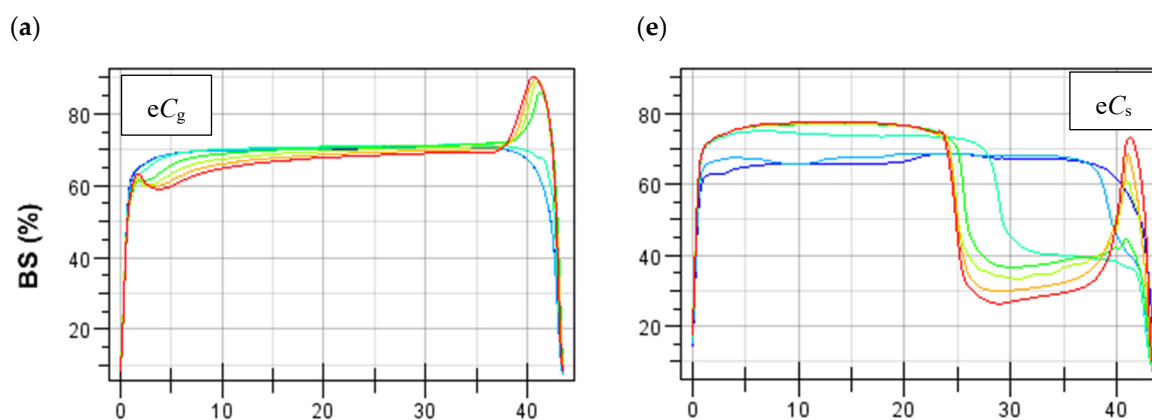


Figure 1. Cont.

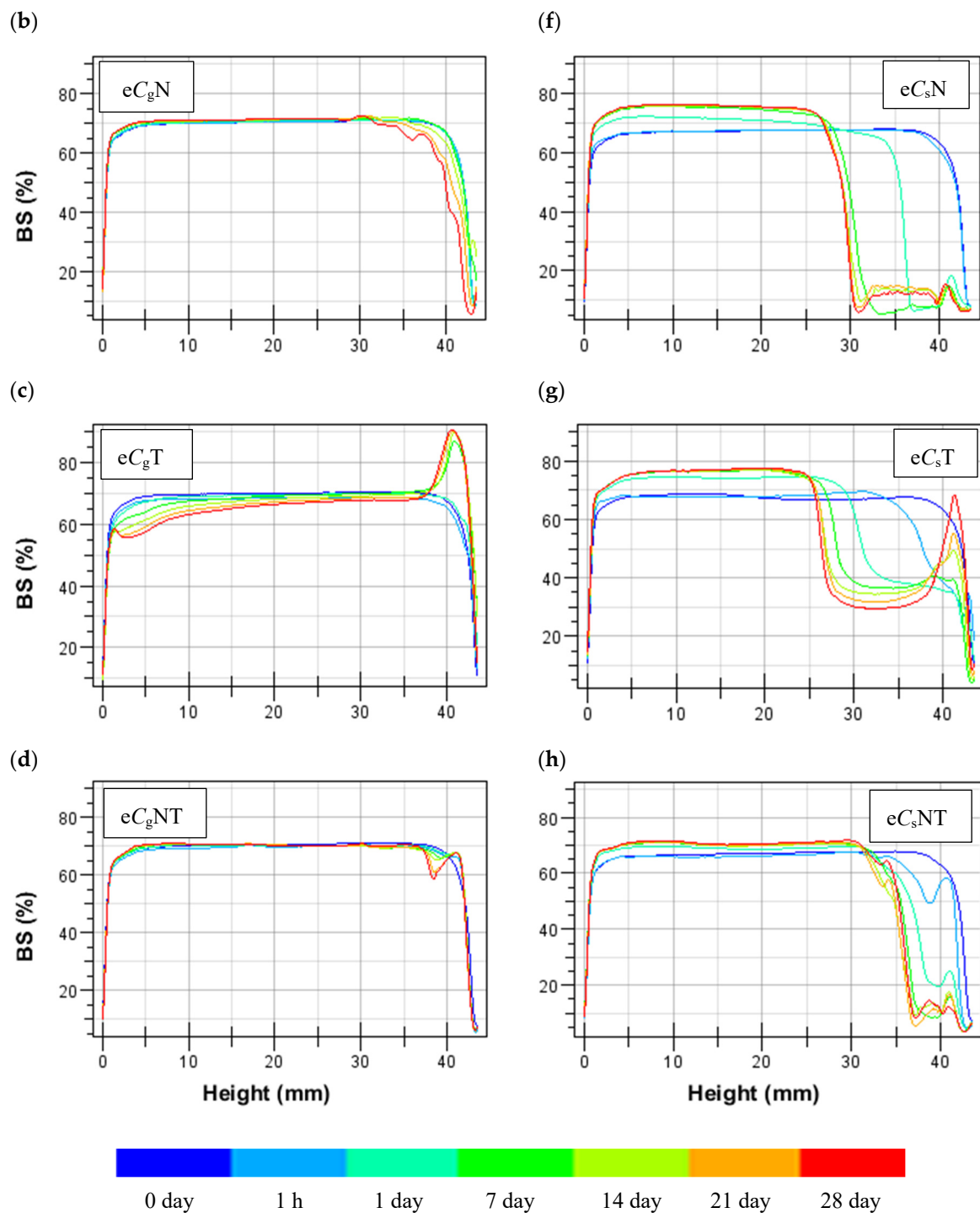


Figure 1. The backscatter (*BS*) profiles of CPC_g - and CPC_s -stabilized emulsions as a function of sample height tested over 28 days, where (a,e) untreated samples (eC_g and eC_s); (b,f) samples with 0.1 M NaCl (eC_gN and eC_sN); (c,g) samples heated to 95 °C (eC_gT and eC_sT); (d,h) samples with 0.1 M NaCl heated to 95 °C (eC_gNT and eC_sNT), respectively.

The stability results for both emulsions were reflected in their PSD data (Table 1) and shear rheological properties (Table 2) as eC_g was low-viscosity Newtonian fluid ($\eta = 3.42 \text{ mPa}\cdot\text{s}$; $n = 1$) with a mean volume diameter below $0.5 \mu\text{m}$, whereas eC_s with a particle size approximately 70 times larger was a non-Newtonian fluid exhibiting the shear-thinning and yield stress (the Herschel–Bulkley model was used to describe the flow curves quantitatively) as well as more than twice the viscosity. Larger particles or their

aggregates under the influence of gravity fell to the bottom of the eC_s, and a thickened emulsion (to a height of approx. 23 mm) was formed (Figure 1e). In turn, upward creaming in eC_s and eC_g was driven by the buoyancy of the emulsion droplets in the continuous phase due to density differences between the dispersed particles and the serum phase. It is a well-known phenomenon in oil-in-water food emulsions as edible oils have lower densities than water [51].

Table 1. The results of the volume PSD (d_{43} and $span$) and Turbiscan Stability Index (TSI) after 1, 7, and 28 days of storage for CPC_g- and CPC_s-stabilized emulsions.

Sample ¹	PSD		Turbiscan Stability ²					
	d_{43} [μm]	$span$ [-]	1. Day		7. Day		28. Day	
			TSI [-]	Category	TSI [-]	Category	TSI [-]	Category
eC _g	0.70 ± 0.02 ^a	3.19 ± 0.08 ^c	0.4 ± 0.0 ^a	A+	3.0 ± 0.1 ^a	B	5.8 ± 0.2 ^a	C
eC _g N	1.10 ± 0.03 ^a	4.64 ± 0.16 ^e	0.1 ± 0.0 ^a	A+	0.7 ± 0.0 ^a	A	2.8 ± 0.2 ^{a,b}	C
eC _g T	0.80 ± 0.00 ^a	3.68 ± 0.07 ^d	0.4 ± 0.2 ^a	A+	2.7 ± 1.0 ^a	B	6.4 ± 0.3 ^a	C
eC _g NT	51.25 ± 0.68 ^c	1.48 ± 0.02 ^a	0.2 ± 0.1 ^a	A+	1.1 ± 0.3 ^a	B	1.7 ± 0.3 ^b	B
eC _s	40.62 ± 0.23 ^b	1.87 ± 0.01 ^{a,b}	12.8 ± 0.2 ^c	D	17.0 ± 0.4 ^b	D	22.1 ± 0.7 ^d	D
eC _s N	36.83 ± 0.81 ^b	2.04 ± 0.05 ^b	6.1 ± 0.7 ^{a,b}	C	29.1 ± 2.8 ^c	D	36.5 ± 1.8 ^e	D
eC _s T	37.77 ± 1.67 ^b	1.99 ± 0.08 ^b	6.8 ± 1.8 ^{b,c}	C	11.5 ± 1.1 ^b	D	17.2 ± 0.0 ^c	D
eC _s NT	38.05 ± 0.22 ^b	1.97 ± 0.01 ^b	5.0 ± 2.4 ^{a,b}	C	11.4 ± 0.8 ^b	D	14.5 ± 0.0 ^c	D

Obtained data are expressed as means ± SD; ^{a,b,c,d,e}—mean values in columns denoted by different letters differ significantly (Tukey's test, $p \leq 0.05$); ¹ eC_g—CPC_g-stabilized emulsion; eC_s—CPC_s-stabilized emulsion; eC_gT and eC_sT—emulsions heated to 95 °C; eC_gN and eC_sN—emulsions with 0.1 M NaCl; eC_gNT and eC_sNT—emulsions with 0.1 M NaCl heated to 95 °C. ² Category of Turbiscan Stability and TSI limits: A+—excellent stability ($TSI < 0.5$), A—good stability ($TSI 0.5-1$), B—satisfactory stability ($TSI 1-3$), C—poor stability ($TSI 3-10$), and D—unsatisfactory stability ($TSI > 10$).

Table 2. The calculated values of viscosity and rheological model parameters derived from fitting the shear curve according to the Newton, Ostwald–de Waele, or Herschel–Bulkley model of the flow behavior for the CPC_g- and CPC_s-stabilized emulsions.

Sample ¹	μ_{100} [§] [mPa·s]	VRI [†] [-]	Model [‡] ($r \geq 0.999$)	μ [mPa·s]	k [mPa·s ⁿ]	N [-]	τ_0 [mPa]
eC _g	3.42 ± 0.22 ^c	0 ± 0.000 ^a	Newton	3.42 ± 0.22	-	1	-
eC _g N	11.26 ± 0.05 ^e	0.341 ± 0.001 ^b	Ostwald–de Waele	-	25.89 ± 0.06	0.819 ± 0.000	-
eC _g T	3.08 ± 0.00 ^{b,c}	0 ± 0.000 ^a	Newton	3.08 ± 0.00	-	1	-
eC _g NT	60.13 ± 0.30 ^f	0.775 ± 0.002 ^e	Herschel–Bulkley	-	326 ± 24	0.573 ± 0.013	1454 ± 83
eC _s	8.73 ± 0.41 ^d	0.531 ± 0.051 ^c	Herschel–Bulkley	-	19.7 ± 4.5	0.810 ± 0.030	60.0 ± 31.7
eC _s N	7.89 ± 0.05 ^d	0.481 ± 0.002 ^c	Herschel–Bulkley	-	16.5 ± 0.7	0.828 ± 0.010	40.9 ± 2.6
eC _s T	8.93 ± 0.65 ^d	0.529 ± 0.001 ^c	Herschel–Bulkley	-	21.7 ± 3.2	0.794 ± 0.015	54.5 ± 1.9
eC _s NT	11.03 ± 0.53 ^e	0.636 ± 0.007 ^d	Herschel–Bulkley	-	36.7 ± 8.1	0.718 ± 0.035	113.2 ± 6.9

Obtained data are expressed as means ± SD; ^{a,b,c,d,e,f}—mean values in columns denoted by different letters differ significantly (Tukey's test, $p \leq 0.05$); ¹ description as in Table 1. [§] μ_{100} —viscosity at shear rate = 100 s⁻¹. [†] The viscosity reduction index (VRI): $VRI = 1 - (\mu_{100}/\mu_{10})$, where μ_{10} —viscosity at shear rate = 10 s⁻¹. [‡] Model: Newton: $\tau = \mu \cdot \dot{\gamma}$; Ostwald–de Waele: $\tau = k \cdot \dot{\gamma}^n$; Herschel–Bulkley: $\tau = \tau_0 + k \cdot \dot{\gamma}^n$, where τ —shear stress, μ —viscosity coefficient, $\dot{\gamma}$ —shear rate, k —consistency index, n —flow index, τ_0 —yield stress; $\tau_0 \geq 0$ and $n < 1$ for a shear-thinning fluid, while $\tau_0 = 0$ and $n = 1$ for a Newtonian fluid.

The three-modal PSD with both fine particles and two fractions of coarse particles in the range of a few to over 100 μm resulted in phenomena such as gravitational separation (creaming and sedimentation), which had a strong impact on the physical stability of eC_s and was unsatisfactory (category D) from the first day (Table 1; Figure S2b). In turn, eC_g with monomodal PSD and fine particles in the range of 0.1 to 1 μm were much more stable

throughout the storage period. Its stability changed over time from excellent after one day of emulsion preparation to poor after 28 days (Table 1; Figure S2a).

3.2.2. Heat- and Salt-Treated CPC-Stabilized Oil-in-Water Emulsions

The method applied for the preparation of the protein powders, including isolation and recovery, affects their functional properties, in particular solubility [14]. In the present study, the commercial CPC powders despite the similar amino profile differed in the pH of their aqueous dispersions. The pH of the standard CPC water dispersion (~6.5) was closer to the *pI* of chickpea proteins (reported as 4.49 [19]) than the pH of gelling CPC (pH~7.5). The pH 7.5 is relatively distant above the *pI* of globulins, which promotes solubility through electrostatic repulsion and hydration of charged residues [20]. Therefore, both the properties and the stability of the emulsions obtained on the basis of these concentrates differed significantly (as described above). It was hypothesized that the influence of external factors on the properties and stability of the emulsion would also be different depending on the concentrate used for their stabilization. The stability of eC_g and eC_s after (a) heating at 95 °C, (b) addition of 0.1 M NaCl, and (c) heating up to 95 °C in the presence of 0.1 M NaCl was examined.

Emulsions Stabilized by Gelling CPC

For eC_g , the presence of salt ions (Na^+Cl^-) had a stabilizing effect on the emulsion ($TSI < 3$ after 28 days of storage) (Table 1), prevented creaming (Figure 1b,d), and reduced the kinetics of destabilization (Figure S2a). Unheated eC_g with 0.1 M NaCl (eC_gN) was shear-thinning ($n < 1$) fluid of higher viscosity than eC_g (Table 2) and possible tendency to flocculation and syneresis manifested by the decrease in *BS* in the upper part of the measuring vial (Figure 1b) with a slight increase in d_{43} and *span* (Table 1). It is a known phenomenon that salt addition produces a progressive increase in viscous and viscoelastic parameters, leading to improved stability against creaming without a significant influence on droplet size distribution [52].

A significant increase in d_{43} (Table 1) and three-modal PSD with the main fraction particles in the range of a few dozen to over 100 μm for eC_g heated in the presence of NaCl (eC_gNT) (Figure S3a) accompanied by stabilization of the system (Figure 1b, Figure S2a) may indicate the formation of the gel structure. This assumption was confirmed by confocal microscopy images of the emulsion. The structure of eC_g significantly changed after heating in the presence of NaCl, extensive droplet aggregation occurred, and a network of aggregated protein-stabilized emulsion droplets was created (Figure S4c). Similar results were presented by Tan et al. [53] for soy protein-stabilized oil-in-water emulsions (pH 7.0) in the presence of 100 mM NaCl and exposed to high temperature (90 °C). Under the combined effect of salt and high temperature, the adsorbed proteins underwent a conformational change that led to increased exposure of non-polar groups. The hydrophobic attraction between the soy protein-coated oil droplets was high enough to overcome the electrostatic repulsion.

In the present study, the network of aggregated protein-stabilized emulsion droplets was created as a result of two mutually reinforcing phenomena: (1) The presence of monovalent ions probably reduced the thickness of the electric double layer around the adsorbed and non-adsorbed proteins and, thus, also reduced the effective repulsion between the negatively charged oil droplets, facilitating aggregation (a relatively high ionic strength, 0.1 M NaCl, was used in these experiments to screen electrostatic effects). (2) Heat denaturation of globular proteins accompanied by the exposure of hydrophobic groups could facilitate depletion flocculation between droplets. Dietary proteins typically unfold and expose non-polar groups above 50 °C leading to protein aggregation and precipitation through hydrophobic and covalent interactions [20]. Ettoumi et al. [54] claimed that chickpea protein concentration above 1.5% promotes depletion flocculation, as the water–oil interface is already saturated by protein molecules. In turn, Joshi and co-workers [55] suggest a concentration of 1% as the interface saturation point in lentil protein-stabilized emulsion

with an oil fraction of 10%. Therefore, it can be assumed that, in the present study, the continuous phase contained a fraction of the non-adsorbed protein, as the oil phase content was fixed at 3.2% with a balanced ratio of protein concentrate to oil (1:1 *w/w*).

In our previous study [33], we have shown that when the whey protein-coated droplets in oil-in-water emulsions (prepared in the same way as eC_s and eC_g) are in close proximity and/or the continuous phase contains a fraction of the non-adsorbed protein, the emulsion gelation may occur. Shear rheological properties indicated that eC_g with 0.1 M NaCl yielded shear-thinning fluids of very high viscosity ($\eta = 60.13$ mPa·s) if it was additionally heated (Table 2). The data were fitted to the Herschel–Bulkley model, and the obtained values of yield stress and consistency index were very high. Also in the case of the chickpea protein dispersion, after heating with 0.1 M NaCl, a similar trend was observed with k and τ_0 having lower values, as well as the viscosity and VRI (Table S2) than those of the corresponding emulsions. The presented results are in accordance with the findings of Jo et al. [56] for systems in which an oil acted as an active filler, and the increased τ_0 and k parameters corresponded to increased resistance to shear and reinforcement of the structure in the continuous phase.

It should be noted that heating alone did not improve the eC_g stability. The *TSI* values of the heated emulsions were slightly higher than those for unheated ones (Table 1, Figure S2a), and the same destabilization mechanism was observed (Figure 1a,c)—creaming during 28 days of storage. Also, the shear rheological properties remained practically unchanged (Table 2), and the eC_g was still a low-viscosity Newtonian fluid after heating with slightly higher d_{43} and *span* values (Table 1). It can be concluded that at high temperatures, despite the unfolding of proteins and the exposure of their hydrophobic parts, the electrostatic repulsion was large enough to overcome attractive interactions between protein molecules enabling the creation of a network of spatial connections. Similar results have been reported previously for soy protein-stabilized emulsions [52].

Emulsions Stabilized by Standard CPC

The unsatisfactory stability of eC_s was initially improved after heat- and/or salt treatment (from D to C category of *TSI* after 1 day) (Table 1). However, the obtained *TSI* values after 7 days (Table 1) and the presented destabilization kinetics (Figure S2b) indicate that in the long term, it was heating (with or without salt) rather than the presence of salt that caused the *TSI* to be lowered. As for eC_g , the addition of 0.1 M NaCl prevented creaming (Figure 1f) and also reduced sedimentation if the emulsion was additionally heated (Figure 1h). However, unheated eC_s with 0.1 M NaCl was the least stable over the 28-day period (Figure S2b). In the presence of salt, a clear layer was formed in the upper part of the emulsions (Figure S5b), which resulted in receiving transmission signals at a height of more than 30 mm (Figure S6a), or more than 36 mm if the emulsion was additionally heated (Figure S6b). The separation of the emulsion in the presence of salt into two phases during storage may indicate dehydration by salting-out. In the presence of dissociated Na^+ and Cl^- ions, the solubility of the protein decreased as a result of competition with salt ions for interaction with the solvent molecules, which led to protein precipitation over a long period of storage.

All eC_s (untreated, heat-treated and/or salt-treated), like heat- and salt-treated eC_g , were shear-thinning fluids with a yield point, but they showed a much lower viscosity, consistency index and yield strength, and a higher flow index, closer to unity (Table 2). Large assemblages of aggregated particles were formed in the emulsions, which were not connected in a spatial network (Figure S4d–f). Single connections between the aggregates could only be formed in the emulsion heated in the presence of salt as a combination of the effect of exposing hydrophobic groups and increasing the attractive forces between them. It is indicated by the highest stability, viscosity and viscosity reduction index, as well as consistency factor and yield point of this emulsion (Figure 1 and Figure S2b, Table 2). However, the values of these parameters were much lower than in the case of corresponding eC_g . Moreover, neither the addition of salt nor the increase in temperature resulted in a

change in PSD (Figure S3b) or an increase in the average particle diameter; on the contrary, d_{43} was lower (Table 1). It can be assumed that external factors influence the intermolecular interactions in the aggregates formed at the emulsion preparation stage more than between the aggregates. A gel structure was not formed.

3.3. Viscoelastic Behavior of CPC-Stabilized Emulsions

In comparison to steady-state flow measurements, the oscillatory (dynamic) measurements can be used to obtain information on the viscoelastic and gel characteristics of protein-stabilized emulsions as it depends on protein denaturation, aggregation, and their conformational changes in the system [45,46].

The thermal gelation process of globular proteins typically involves two main steps: (1) heat-induced unfolding of the native protein structure by exposing the interaction sites and (2) intermolecular aggregation of unfolded proteins into a spatial network [33,57]. The physical gelation behavior of protein dispersions can be studied *via* rheology, where the bulk viscoelastic properties can be used to examine the transition from a liquid state to a solid-like gel. Overall, the thermal gelation of globular proteins in the emulsion is a complex physicochemical process driven by various inter- and intramolecular interactions. We assumed that, using rheological data, conformational changes during the thermal gelation process of proteins can be directly correlated with the increases in bulk viscoelastic properties, both for the CPC-stabilized oil-in-water emulsion and for the CPC water dispersion. The viscoelasticity of the tested systems was analyzed by studying the storage (G') and loss modulus (G'') at a constant oscillation frequency and strain amplitude during heating from 20 to 95 °C, holding at 95 °C, and then cooling to 20 °C. Before heating, the emulsions and their water dispersions were held at 20 °C.

3.3.1. Emulsions Stabilized by Gelling CPC

The CPC_g-stabilized emulsions and CPC_g dispersion at 20 °C behaved as free-flowing viscous liquids, where G'' was greater than G' , and both moduli remained steady at constant temperature (Figure 2).

To initiate the heat-induced gelation process in eC_g the temperature was increased from 20 °C to 95 °C at a rate of 4 °C/min. Initially, both G' and G'' began to decrease as the overall viscosity of the emulsion decreased with increasing temperature. However, when the temperature reached ~72 °C (after approx. 12 min of heating), both G' and G'' began to increase rapidly (Figure 2b). Such an increase in moduli values may suggest that the observed rheological behavior was directly related to the denaturation of the chickpea protein molecules. As a result of heat treatment (at 95 °C for 15 min), their globular conformation was irreversibly changed to a more random structure by exposure to previously buried hydrophobic groups leading to protein aggregation.

Dent et al. [58] indicated the presence of a broad denaturation peak in the range of ~65–100 °C with a maximum at 90 °C on the DSC thermogram of an unhydrolyzed chickpea protein isolate. Papalamprou et al. [14] reported broad endothermic transition in the DSC scans of three chickpea protein isolates (20% *w/v* protein dispersion, pH 7) with the onset around 78–80 °C or 57 °C and the peak denaturation temperature values of 97–103 °C or 92 °C, respectively, depending on the method applied for their preparation. According to the authors, endothermic troughs in DSC thermograms were the result of overlapping thermal denaturation events of legumin and vicilin proteins in the former and those of the albumin fraction in the latter. It can be stated that the slight increase in G' and G'' around 55 °C could be attributed to the beginning of conformational changes for albumin fraction as a result of heating.

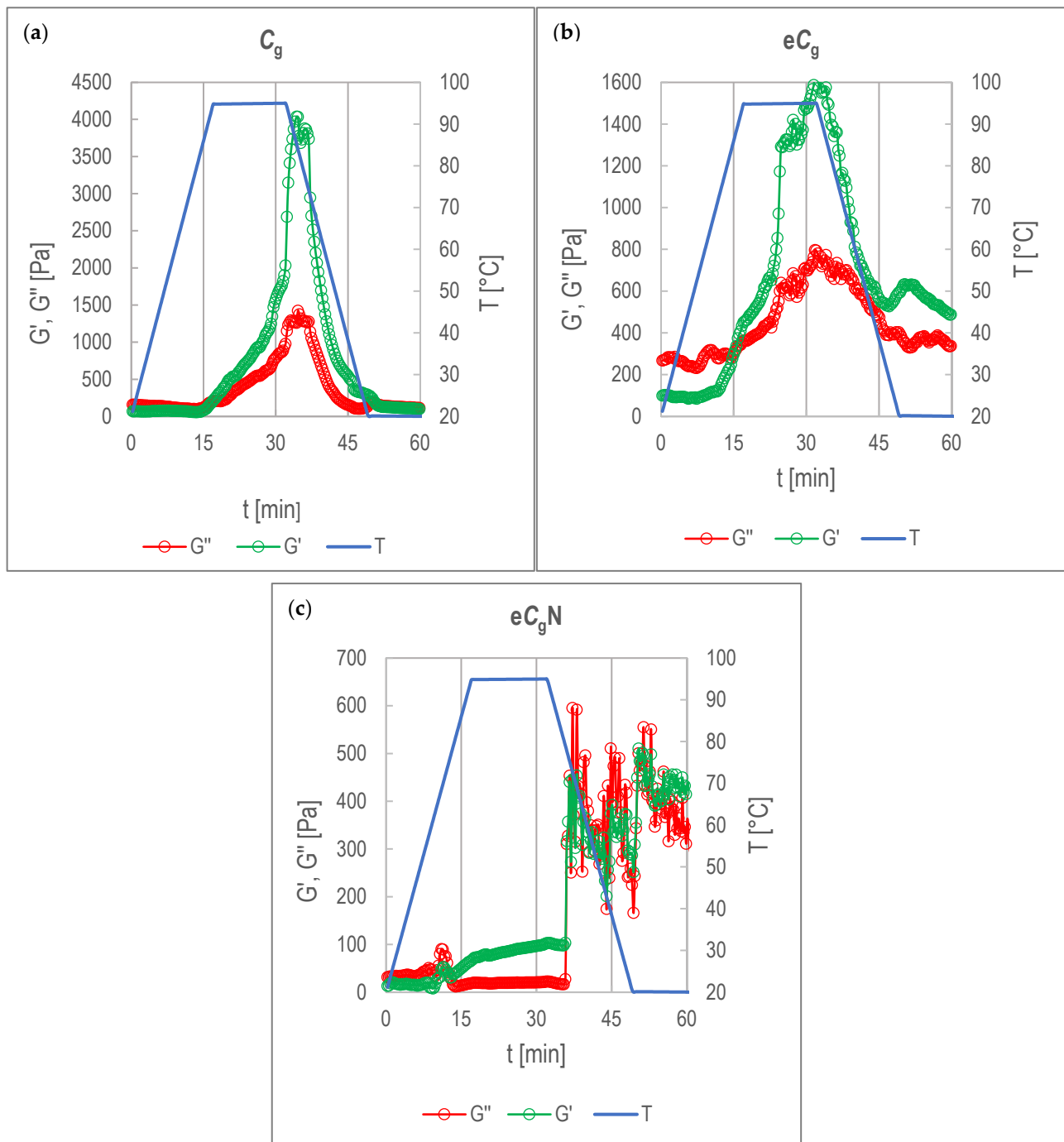


Figure 2. Elastic modulus (G') and viscous modulus (G'') plotted vs. time for CPC_g dispersion (C_g) (a), CPC_g -stabilized emulsion (eC_g) (b), and CPC_g -stabilized emulsion with 0.1M NaCl (eC_gN) (c) during the temperature ramp-up, hold, and ramp-down procedure.

Once the temperature reached 95 °C, G' was now significantly greater than G'' (i.e., a crossover was observed at 86 °C), indicating that the emulsion had transformed from a liquid into a solid-like state during the increasing temperature ramp. Then, during the isothermal hold step at 95 °C (17–32 min), G' and G'' continued to increase even though the temperature remained constant; however, G' began to increase at a slower rate during the second half of the isothermal hold at 95 °C. The increase in G' during gelation can be attributed to the formation of filamentous or fine-stranded aggregates. Previous studies have shown that (1) prolonged heating at 90 °C not only accelerates protein aggregation

rates but also leads to the rapid formation of firmly structured gels and an overall more elastic gel network [59,60]; (2) gelation of globular proteins at low ionic strength and $pI < pH < pI$ produces fine-stranded gel [61].

Then, as the temperature was decreased back to 20 °C, both G' and G'' began to decrease rapidly. During the cooling step, G' decreased but further deviated from G'' , indicating the maintenance of the structural change in which the sample transitioned into an elastically dominated system ($G' > G''$). When the temperature returned to 20 °C, a significant difference in the initial and final G' values was clearly evident (Figure 2b), suggesting that permanent heat-induced conformational changes of the protein had occurred. The increase in elasticity of the system (denoted by the rise in G') was most likely due to the non-covalent interactions such as hydrogen bonds and hydrophobic interactions [59,62,63]. Nevertheless, the observed decrease in viscoelasticity as the temperature decreased suggests the formation of a fine-stranded gel in which heat-induced protein gelation involved unfolding followed by protein aggregation but not spatial cross-linking (covalent bonds were not significantly involved in the gel structure). Under these conditions, biopolymer molecules built up thin filaments and had a low tendency to aggregate further; protein molecules did not undergo extensive aggregation owing to the strong electrostatic repulsion between them.

In the case of the C_g , changes in G' and G'' were also observed during the temperature ramp-up, hold, and ramp-down procedure (Figure 2a). The increase in G' and G'' started when the temperature reached ~82 °C (14 min) and continued when the temperature was held constant at 95 °C, indicating molecular unfolding (denaturation). Then, when lowering the temperature back to 20 °C, the G' and G'' also decreased. Finally, once the temperature returned to 20 °C, the decrease in moduli plateaued, and the specimen reached its final $G' < G''$, suggesting its liquid state remains similar to before heating. It should be mentioned that a higher denaturation temperature of proteins in their water dispersion compared to the denaturation temperature in emulsion has also been demonstrated for other protein systems, because proteins undergoing surface denaturation during adsorption at the water–oil interface are more susceptible to thermal denaturation [33,34,64].

For eC_g with 0.1M NaCl, peaks of G' and G'' moduli were observed at ~72 °C (12 min) during heating (Figure 2c). As the temperature was further ramped, G' was now significantly greater than G'' (i.e., a crossover was observed), and the increase in G'' began to slow down. Then, during the isothermal hold step at 95 °C, G' increased until the end of the ramp, and G'' remained fairly constant. The increase in G' upon heating suggests that the observed rheological behavior was driven by conformational changes and aggregation of the protein molecules. During the cooling step, a sudden increase in both G' and G'' initiated at 80 °C, and then rapid jumps in the rheological responses were observed. It suggests that protein aggregation and the growth and rearrangement of aggregates were induced and further accentuated when the temperature was reached and lowered. In the presence of NaCl, aggregation was more random leading to particulate aggregates linked together in a spatial network (Figure S4c). Presented results are in accordance with previous findings that (1) extended heating at 90 °C with addition of NaCl accelerates protein aggregation rates, leading to the formation of more aggregated gel structures [59,62]; (2) external conditions that decrease electrostatic repulsion, such as increased ionic strength or $pH \sim pI$, promote the further aggregation of the primary aggregates, causing a coarsening of the network that results in a particulate structure (particulate gel) [61].

3.3.2. Emulsions Stabilized by Standard CPC

In the case of C_s as well as eC_s , both with and without 0.1 M NaCl, changes in G' and G'' were also observed during heat treatment (Figure 3), but the relationship between G' and G'' at individual stages of thermal treatment differed from that for the corresponding systems with gelling CPC. The C_s and eC_s during the temperature ramp up and hold showed the increase in G' and G'' , which was induced at about 85 °C for protein water dispersion and at ~70 °C for emulsion (Figures 3a and 3b, respectively), and during the

ramp-down procedure, a decrease in moduli was observed. What is important is that the G' and G'' moduli curves intersected twice. The first time was due to the formation of a viscoelastic structure at the holding stage and then at the cooling stage ($\sim 56^\circ\text{C}$ for C_s and $\sim 70^\circ\text{C}$ for eC_s) as a result of gel–sol transition. Probably, only reversible, weak, and long-distance interactions were responsible for aggregation and gel formation.

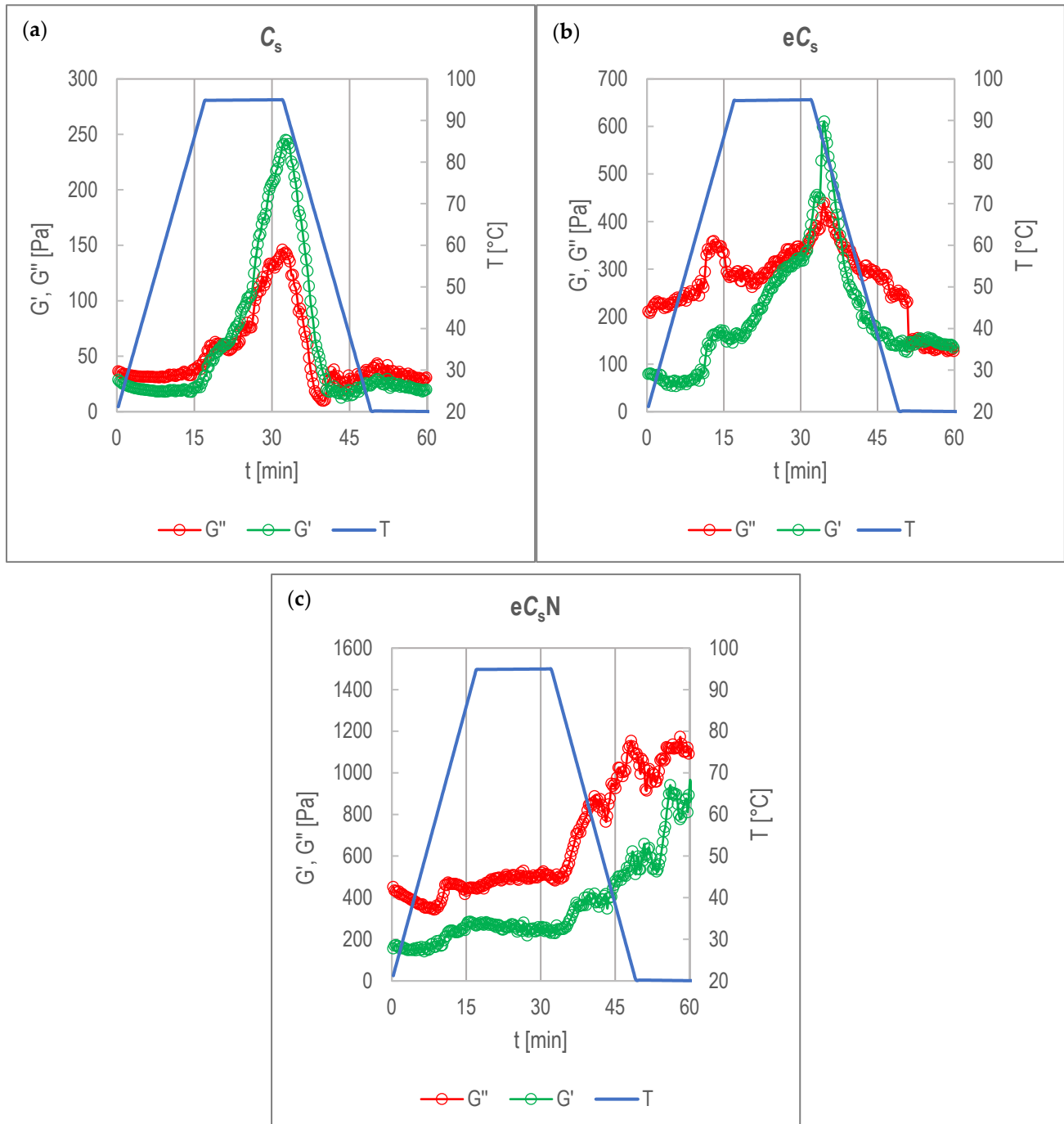


Figure 3. Elastic modulus (G') and viscous modulus (G'') plotted vs. time for CPC_s dispersion (C_s) (a), CPC_s -stabilized emulsion (eC_s) (b), and CPC_s -stabilized emulsion with 0.1M NaCl (eC_sN) (c) during the temperature ramp-up, hold, and ramp-down procedure.

For eC_s with 0.1 M NaCl, the significant increase in G' and G'' was induced at $\sim 70^\circ\text{C}$, the moduli remained fairly constant (with a slight decrease in G') during the isothermal hold step at 95°C , and then they started to increase once again but at a significantly faster

rate during the decreasing temperature ramp to 20 °C. Ultimately, G'' was significantly greater than G' at all stages of heat treatment, indicating that even prolonged heating of eC_s with 0.1 M NaCl at 95 °C did not lead to gel formation.

4. Conclusions

Food processing may lead to changes in the structure and functionality of proteins. Understanding these changes is crucial when selecting protein powders for specific applications. The presented findings indicate that the type of chickpea concentrate used as an emulsion stabilizer (standard CPC and gelling CPC) has a significant impact on the stability and rheological behavior of the emulsion. Moreover, it determines the functionality of the protein-stabilized emulsion (e.g., its tendency to gel), particularly in combination with environmental conditions (heat- and/or salt treatment).

The gelling CPC produced a fine, homogeneous emulsion with an average particle size $< 1 \mu\text{m}$ and Newtonian behavior that formed a heat-induced gel. However, gelation was accompanied by emulsion stabilization and a significant change in both shear rheological properties and particle size distribution, only in the presence of salt. The heat- (95 °C) and salt (0.1 M NaCl) treatment lead to the formation of a coarsely aggregated particulate gel.

Emulsions stabilized with standard CPC (eC_s) were unstable non-Newtonian fluids due to large particle sizes. eC_s formed a thermoreversible viscoelastic structure during heat treatment. The addition of 0.1M NaCl improved the physical stability of the eC_s when it was accompanied by heat treatment; but in this case, no gel structure was formed.

The selection of the protein powders and their processing conditions is of key importance, among others, in modeling functional food matrices, especially in the field of creating protein-based delivery systems for nutraceuticals.

Supplementary Materials: The following supporting information can be downloaded at <https://www.mdpi.com/article/10.3390/app14072698/s1>, Figure S1: The PSD graphs (cumulative and histogram) for CPC_s and CPC_g dispersions (C_s and C_g), pre-processed once (^{one}HPH) or twice (^{two}HPH) in high-pressure two-stage homogenizer (a) and for corresponding emulsions, eC_s and eC_g , obtained from these dispersions (b); Figure S2: The Turbiscan Stability Index (TSI) kinetics of global destabilization for CPC_g - and CPC_s -stabilized emulsion (a and b, respectively), where eC_g and eC_s —untreated samples; eC_gN and eC_sN —samples with 0.1 M NaCl; eC_gT and eC_sT —sample heated to 95 °C; eC_gNT and eC_sNT —samples with 0.1M NaCl heated to 95 °C; Figure S3: The PSD graphs (cumulative and histogram) for CPC_g - and CPC_s -stabilized emulsions (a and b, respectively), where eC_g and eC_s —untreated samples; eC_gN and eC_sN —samples with 0.1M NaCl; eC_gT and eC_sT —samples heated to 95 °C; eC_gNT and eC_sNT —samples with 0.1M NaCl heated to 95 °C; Figure S4: CLSM images of CPC_g -stabilized emulsions (a–c) and CPC_s -stabilized emulsions (d–f), where (a,d) untreated emulsions; (b,e) emulsions heated to 95 °C; (c,f) emulsions with 0.1 M NaCl heated to 95 °C. The green regions represent lipids and blue means the protein. The scale bar is 20 μm ; Figure S5: Photographs of CPC_g - and CPC_s -stabilized emulsion (a and b, respectively) after storage, where eC_g and eC_s —untreated samples; eC_gN and eC_sN —samples with 0.1M NaCl; eC_gT and eC_sT —sample heated to 95 °C; eC_gNT and eC_sNT —samples with 0.1M NaCl heated to 95 °C. Emulsions are presented in Turbiscan glass cells; Figure S6: The transmission (%T) as a function of sample height for eC_s during storage within 28 days: sample with 0.1 M NaCl (a), sample with 0.1M NaCl heated to 95 °C (b); Table S1: The results of the volume PSD (d_{10} , d_{50} , d_{90} , and *span*) for CPC_g and CPC_s dispersions after once and twice passing through the high-pressure homogenizer and for emulsions prepared from these dispersions; Table S2: The calculated values of viscosity and rheological model parameters derived from fitting the shear curve according to the Newton, Ostwald–de Waele, or Herschel–Bulkley model of the flow behavior for the CPC_g and CPC_s dispersions.

Author Contributions: Conceptualization, D.M.-J. and E.D.; methodology, D.M.-J. and E.D.; software, E.D.; validation, D.M.-J. and E.D.; formal analysis, D.M.-J. and E.D.; investigation, D.M.-J. and E.D.; resources, E.D.; data curation, D.M.-J. and E.D.; writing—original draft preparation, D.M.-J.; writing—review and editing, D.M.-J. and E.D.; visualization, D.M.-J. and E.D.; supervision, E.D.; project administration, D.M.-J. and E.D.; funding acquisition, D.M.-J. and E.D. All authors have read and agreed to the published version of the manuscript.

Funding: This research received no external funding.

Institutional Review Board Statement: Not applicable.

Informed Consent Statement: Not applicable.

Data Availability Statement: The data presented in this study are available in article.

Conflicts of Interest: The authors declare no conflicts of interest.

References

1. Glusac, J.; Isaschar-Ovdat, S.; Fishman, A. Transglutaminase modifies the physical stability and digestibility of chickpea protein-stabilized oil-in-water emulsions. *Food Chem.* **2020**, *315*, 126301. [[CrossRef](#)]
2. Goldstein, N.; Reifen, R. The potential of legume-derived proteins in the food industry. *Grain Oil Sci. Technol.* **2022**, *5*, 167–178. [[CrossRef](#)]
3. Zhang, S.; Holmes, M.; Ettlalaie, R.; Sarkar, A. Pea protein microgel particles as Pickering stabilisers of oil-in-water emulsions: Responsiveness to pH and ionic strength. *Food Hydrocoll.* **2020**, *102*, 105583. [[CrossRef](#)]
4. Semba, R.D.; Ramsing, R.; Rahman, N.; Kraemer, K.; Bloem, M.W. Legumes as a sustainable source of protein in human diets. *Glob. Food Secur.* **2021**, *28*, 100520. [[CrossRef](#)]
5. Gundogan, R.; Tomar, G.S.; Karaca, A.C.; Capanoglu, E.; Tulbek, M.C. Chapter 9—Chickpea Protein: Sustainable Production, Functionality, Modification, and Applications. In *Sustainable Protein Sources*, 2nd ed.; Nadathur, S., Janitha, P.D., Wanasundara, L.S., Eds.; Academic Press: Cambridge, MA, USA, 2024; pp. 185–199. [[CrossRef](#)]
6. He, Y.; Meda, V.; Reaney, M.J.; Mustafa, R. Aquafaba, a new plant-based rheological additive for food applications. *Trends Food Sci. Technol.* **2021**, *111*, 27–42. [[CrossRef](#)]
7. Onyango, E. Legume Protein: Properties and Extraction for Food Applications. In *Legumes Research—Volume 2*; Jimenez-Lopez, J.C., Clemente, A., Eds.; IntechOpen: London, UK, 2022. [[CrossRef](#)]
8. Boukid, F. Chickpea (*Cicer arietinum* L.) protein as a prospective plant-based ingredient: A review. *Int. J. Food Sci. Technol.* **2021**, *56*, 5435–5444. [[CrossRef](#)]
9. Shakoor, I.F.; Pamunuwa, G.K.; Karunaratne, D.N. Chickpea and soybean protein delivery systems for oral ingestion of hydroxycitric acid. *Food Chem. Adv.* **2023**, *2*, 100207. [[CrossRef](#)]
10. Begum, N.; Khan, Q.U.; Liu, L.G.; Li, W.; Liu, D.; Haq, I.U. Nutritional composition, health benefits and bio-active compounds of chickpea (*Cicer arietinum* L.). *Front. Nutr.* **2023**, *10*, 1218468. [[CrossRef](#)]
11. Patil, N. Chickpea protein: A comprehensive review on nutritional properties, processing, functionality, applications, and sustainable impact. *Pharm. Innov. J.* **2023**, *12*, 3424–3434.
12. Chang, L.; Lan, Y.; Bandillo, N.; Ohm, J.-B.; Chen, B.; Rao, J. Plant proteins from green pea and chickpea: Extraction, fractionation, structural characterization and functional properties. *Food Hydrocoll.* **2022**, *123*, 107165. [[CrossRef](#)]
13. Grasso, N.; Lynch, N.L.; Arendt, E.K.; O'Mahony, J.A. Chickpea protein ingredients: A review of composition, functionality, and applications. *Compr. Rev. Food Sci. Food Saf.* **2022**, *21*, 435–452. [[CrossRef](#)]
14. Papalamprou, E.; Doxastakis, G.; Biliaderis, C.; Kiosseoglou, V. Influence of preparation methods on physicochemical and gelation properties of chickpea protein isolates. *Food Hydrocoll.* **2009**, *23*, 337–343. [[CrossRef](#)]
15. Ramani, A.; Kushwaha, R.; Malaviya, R.; Kumar, R.; Yadav, N. Molecular, functional and nutritional properties of chickpea (*Cicer arietinum* L.) protein isolates prepared by modified solubilization methods. *J. Food Meas. Charact.* **2021**, *15*, 2352–2368. [[CrossRef](#)]
16. Felix, M.; Cermeño, M.; Romero, A.; FitzGerald, R.J. Characterisation of the bioactive properties and microstructure of chickpea protein-based oil in water emulsions. *Food Res. Int.* **2019**, *121*, 577–585. [[CrossRef](#)] [[PubMed](#)]
17. Johnston, S.P.; Nickerson, M.T.; Low, N.H. The physicochemical properties of legume protein isolates and their ability to stabilize oil-in-water emulsions with and without genipin. *J. Food Sci. Technol.* **2015**, *52*, 4135–4145. [[CrossRef](#)] [[PubMed](#)]
18. Karaca, A.C.; Low, N.; Nickerson, M. Emulsifying properties of chickpea, faba bean, lentil and pea proteins produced by isoelectric precipitation and salt extraction. *Food Res. Int.* **2011**, *44*, 2742–2750. [[CrossRef](#)]
19. Karaca, A.C.; Nickerson, M.T.; Low, N.H. Lentil and Chickpea Protein-Stabilized Emulsions: Optimization of Emulsion Formulation. *J. Agric. Food Chem.* **2011**, *59*, 13203–13211. [[CrossRef](#)] [[PubMed](#)]
20. Bogahawaththa, D.; Chau, N.H.B.; Trivedi, J.; Dissanayake, M.; Vasiljevic, T. Impact of selected process parameters on solubility and heat stability of pea protein isolate. *LWT* **2019**, *102*, 246–253. [[CrossRef](#)]
21. Grossmann, L.; McClements, D.J. Current insights into protein solubility: A review of its importance for alternative proteins. *Food Hydrocoll.* **2023**, *137*, 108416. [[CrossRef](#)]
22. Keuleyan, E.; Gélébart, P.; Beaumal, V.; Kermarrec, A.; Ribourg-Birault, L.; Le Gall, S.; Meynier, A.; Riaublanc, A.; Berton-Carabin, C. Pea and lupin protein ingredients: New insights into endogenous lipids and the key effect of high-pressure homogenization on their aqueous suspensions. *Food Hydrocoll.* **2023**, *141*, 108671. [[CrossRef](#)]
23. Kaur, M.; Singh, N. Characterization of protein isolates from different Indian chickpea (*Cicer arietinum* L.) cultivars. *Food Chem.* **2007**, *102*, 366–374. [[CrossRef](#)]
24. Novák, P.; Havlíček, V. 4—Protein Extraction and Precipitation. In *Proteomic Profiling and Analytical Chemistry*; Ciborowski, P., Silberring, J., Eds.; Elsevier: Amsterdam, The Netherlands, 2016; pp. 51–62. [[CrossRef](#)]

25. Yousefi, N.; Abbasi, S. Food proteins: Solubility & thermal stability improvement techniques. *Food Chem. Adv.* **2022**, *1*, 100090. [[CrossRef](#)]
26. Ben-Harb, S.; Panouillé, M.; Huc-Mathis, D.; Moulin, G.; Saint-Eve, A.; Irlinger, F.; Bonnarme, P.; Michon, C.; Souchon, I. The rheological and microstructural properties of pea, milk, mixed pea/milk gels and gelled emulsions designed by thermal, acid, and enzyme treatments. *Food Hydrocoll.* **2018**, *77*, 75–84. [[CrossRef](#)]
27. Gomes, A.; Sobral, P.J.D.A. Plant Protein-Based Delivery Systems: An Emerging Approach for Increasing the Efficacy of Lipophilic Bioactive Compounds. *Molecules* **2022**, *27*, 60. [[CrossRef](#)]
28. Bußler, S.; Steins, V.; Ehlbeck, J.; Schlüter, O. Impact of thermal treatment versus cold atmospheric plasma processing on the techno-functional protein properties from *Pisum sativum* ‘Salamanca’. *J. Food Eng.* **2015**, *167*, 166–174. [[CrossRef](#)]
29. Liu, H.; Zhang, H.; Liu, Q.; Chen, Q.; Kong, B. Solubilization and stable dispersion of myofibrillar proteins in water through the destruction and inhibition of the assembly of filaments using high-intensity ultrasound. *Ultrason. Sonochemistry* **2020**, *67*, 105160. [[CrossRef](#)] [[PubMed](#)]
30. Song, X.; Zhou, C.; Fu, F.; Chen, Z.; Wu, Q. Effect of high-pressure homogenization on particle size and film properties of soy protein isolate. *Ind. Crop. Prod.* **2013**, *43*, 538–544. [[CrossRef](#)]
31. Saricaoglu, F.T. Application of high-pressure homogenization (HPH) to modify functional, structural and rheological properties of lentil (*Lens culinaris*) proteins. *Int. J. Biol. Macromol.* **2020**, *144*, 760–769. [[CrossRef](#)]
32. Yang, J.; Liu, G.; Zeng, H.; Chen, L. Effects of high pressure homogenization on faba bean protein aggregation in relation to solubility and interfacial properties. *Food Hydrocoll.* **2018**, *83*, 275–286. [[CrossRef](#)]
33. Domian, E.; Mańko-Jurkowska, D. The effect of homogenization and heat treatment on gelation of whey proteins in emulsions. *J. Food Eng.* **2022**, *319*, 110915. [[CrossRef](#)]
34. Domian, E.; Mańko-Jurkowska, D.; Górska, A. Heat-induced gelation, rheology and stability of oil-in-water emulsions prepared with patatin-rich potato protein. *Food Bioprod. Process.* **2023**, *139*, 144–156. [[CrossRef](#)]
35. Pan, Y.; Xu, Y.; Zhu, L.; Liu, X.; Zhao, G.; Wang, S.; Yang, L.; Ma, T.; Liu, H. Stability and rheological properties of water-in-oil (W/O) emulsions prepared with a soyasaponin-PGPR system. *Futur. Foods* **2021**, *4*, 100096. [[CrossRef](#)]
36. Xu, D.; Zhang, J.; Cao, Y.; Wang, J.; Xiao, J. Influence of microcrystalline cellulose on the microrheological property and freeze-thaw stability of soybean protein hydrolysate stabilized curcumin emulsion. *LWT* **2016**, *66*, 590–597. [[CrossRef](#)]
37. Håkansson, A. Emulsion Formation by Homogenization: Current Understanding and Future Perspectives. *Annu. Rev. Food Sci. Technol.* **2019**, *10*, 239–258. [[CrossRef](#)] [[PubMed](#)]
38. Mulla, M.Z.; Subramanian, P.; Dar, B. Functionalization of legume proteins using high pressure processing: Effect on technofunctional properties and digestibility of legume proteins. *LWT* **2022**, *158*, 113106. [[CrossRef](#)]
39. Juttulapa, M.; Piriyaarasarth, S.; Takeuchi, H.; Sriamornsak, P. Effect of high-pressure homogenization on stability of emulsions containing zein and pectin. *Asian J. Pharm. Sci.* **2017**, *12*, 21–27. [[CrossRef](#)] [[PubMed](#)]
40. Kuhn, K.; Cunha, R. Flaxseed oil—Whey protein isolate emulsions: Effect of high pressure homogenization. *J. Food Eng.* **2012**, *111*, 449–457. [[CrossRef](#)]
41. Melchior, S.; Moretton, M.; Calligaris, S.; Manzocco, L.; Nicoli, M.C. High pressure homogenization shapes the techno-functionalities and digestibility of pea proteins. *Food Bioprod. Process.* **2022**, *131*, 77–85. [[CrossRef](#)]
42. Subasi, B.G.; Yildirim-Elikoğlu, S.; Altay, I.; Jafarpour, A.; Casanova, F.; Mohammadifar, M.A.; Capanoglu, E. Influence of non-thermal microwave radiation on emulsifying properties of sunflower protein. *Food Chem.* **2021**, *372*, 131275. [[CrossRef](#)] [[PubMed](#)]
43. Kowalska, M.; Krztoń-Maziopa, A.; Babut, M.; Mitrosz, P. Rheological and physical analysis of oil-water emulsion based on enzymatic structured fat. *Rheol. Acta* **2020**, *59*, 717–726. [[CrossRef](#)]
44. Maphosa, Y.; Jideani, V.A. Factors Affecting the Stability of Emulsions Stabilised by Biopolymers. In *Science and Technology behind Nanoemulsions*; Karakus, S., Ed.; IntechOpen: London, UK, 2018; pp. 65–81.
45. Erçelebi, E.A.; Imanoğlu, E. Rheological properties of whey protein isolate stabilized emulsions with pectin and guar gum. *Eur. Food Res. Technol.* **2009**, *229*, 281–286. [[CrossRef](#)]
46. Félix, M.; Carrera, C.; Romero, A.; Bengoechea, C.; Guerrero, A. Rheological approaches as a tool for the development and stability behaviour of protein-stabilized emulsions. *Food Hydrocoll.* **2020**, *104*, 105719. [[CrossRef](#)]
47. Ravera, F.; Dziza, K.; Santini, E.; Cristofolini, L.; Liggieri, L. Emulsification and emulsion stability: The role of the interfacial properties. *Adv. Colloid Interface Sci.* **2021**, *288*, 102344. [[CrossRef](#)] [[PubMed](#)]
48. Tadros, T.F. Emulsion Formation, Stability, and Rheology. In *Emulsion Formation and Stability*; Tadros, T.F., Ed.; Wiley: Hoboken, NJ, USA, 2013; pp. 1–75. [[CrossRef](#)]
49. Niu, H.; Wang, W.; Dou, Z.; Chen, X.; Chen, X.; Chen, H.; Fu, X. Multiscale combined techniques for evaluating emulsion stability: A critical review. *Adv. Colloid Interface Sci.* **2023**, *311*, 102813. [[CrossRef](#)] [[PubMed](#)]
50. Zamani, Z.; Razavi, S.M.A. Steady shear rheological properties, microstructure and stability of water in water emulsions made with basil seed gum and waxy corn starch or high pressure-treated waxy corn starch. *LWT* **2023**, *174*, 114453. [[CrossRef](#)]
51. Pathak, M. Chapter 5—Nanoemulsions and Their Stability for Enhancing Functional Properties of Food Ingredients. In *Nanotechnology Applications in Food*; Opera, A.E., Grumezescu, A.M., Eds.; Academic Press: Cambridge, MA, USA, 2017; pp. 87–106. [[CrossRef](#)]

52. Martínez, I.; Riscardo, M.A.; Franco, J.M. Effect of salt content on the rheological properties of salad dressing-type emulsions stabilized by emulsifier blends. *J. Food Eng.* **2007**, *80*, 1272–1281. [[CrossRef](#)]
53. Tan, Y.; Lee, P.W.; Martens, T.D.; McClements, D.J. Comparison of Emulsifying Properties of Plant and Animal Proteins in Oil-in-Water Emulsions: Whey, Soy, and RuBisCo Proteins. *Food Biophys.* **2022**, *17*, 409–421. [[CrossRef](#)]
54. Ettoumi, Y.L.; Chibane, M.; Romero, A. Emulsifying properties of legume proteins at acidic conditions: Effect of protein concentration and ionic strength. *LWT* **2016**, *66*, 260–266. [[CrossRef](#)]
55. Joshi, M.; Adhikari, B.; Aldred, P.; Panozzo, J.; Kasapis, S.; Barrow, C. Interfacial and emulsifying properties of lentil protein isolate. *Food Chem.* **2012**, *134*, 1343–1353. [[CrossRef](#)]
56. Jo, M.; Chang, M.J.; Goh, K.K.T.; Ban, C.; Choi, Y.J. Rheology, Microstructure, and Storage Stability of Emulsion-Filled Gels Stabilized Solely by Maize Starch Modified with Octenyl Succinylation and Pregelatinization. *Foods* **2021**, *10*, 837. [[CrossRef](#)]
57. Totosaus, A.; Montejano, J.G.; Salazar, J.A.; Guerrero, I. A review of physical and chemical protein-gel induction. *Int. J. Food Sci. Technol.* **2002**, *37*, 589–601. [[CrossRef](#)]
58. Dent, T.; Campanella, O.; Maleky, F. Enzymatic hydrolysis of soy and chickpea protein with Alcalase and Flavourzyme and formation of hydrogen bond mediated insoluble aggregates. *Curr. Res. Food Sci.* **2023**, *6*, 100487. [[CrossRef](#)] [[PubMed](#)]
59. Badii, F.; Atri, H.; Dunstan, D.E. The effect of shear on the rheology and structure of heat-induced whey protein gels. *Int. J. Food Sci. Technol.* **2016**, *51*, 1570–1577. [[CrossRef](#)]
60. Phillips, L.G.; Whitehead, D.M.; Kinsella, J. *Structure–Function Properties of Food Proteins*; Academic Press: New York, NY, USA, 1994.
61. Foegeding, E.A. Food Biophysics of Protein Gels: A Challenge of Nano and Macroscopic Proportions. *Food Biophys.* **2006**, *1*, 41–50. [[CrossRef](#)]
62. Ramos, L.; Pereira, J.O.; Silva, S.I.; Amorim, M.M.; Fernandes, J.C.; Lopes-Da-Silva, J.A.; Pintado, M.E.; Malcata, F.X. Effect of composition of commercial whey protein preparations upon gelation at various pH values. *Food Res. Int.* **2012**, *48*, 681–689. [[CrossRef](#)]
63. Al-Ali, H.A.; Shah, U.; Hackett, M.J.; Gulzar, M.; Karakyriakos, E.; Johnson, S.K. Technological strategies to improve gelation properties of legume proteins with the focus on lupin. *Innov. Food Sci. Emerg. Technol.* **2021**, *68*, 102634. [[CrossRef](#)]
64. McClements, D.J. Protein-stabilized emulsions. *Curr. Opin. Colloid Interface Sci.* **2004**, *9*, 305–313. [[CrossRef](#)]

Disclaimer/Publisher’s Note: The statements, opinions and data contained in all publications are solely those of the individual author(s) and contributor(s) and not of MDPI and/or the editor(s). MDPI and/or the editor(s) disclaim responsibility for any injury to people or property resulting from any ideas, methods, instructions or products referred to in the content.